Dynamic aeroelastic simulation of composite wing for HALE UAV application

Bertrand Kirsch[⋆]*, Olivier Montagnier*[⋆†]*, Emmanuel Bénard,*[⋆⋆]*, Thierry M. Faure*[⋆]

[⋆]*Centre de Recherche de l'Armée de l'air*
École de l'air, BA 701, F-13661 Salon air, France
bertrand.kirsch@defense.gouv.fr · olivier.montagnier@defense.gouv.fr · thierry.faure@defense.gouv.fr

[⋆⋆]*Département Conception et conduite des véhicules Aéronautiques et Saptiaux (DCAS)*
Institut Supérieur de l'Aéronautique et de l'Espace - Supaéro
10 avenue Édouard Belin, BP 54032 - 31055 Toulouse CEDEX 4, France
emmanuel.benard@isae.fr

[†]*Aix Marseille Univ, CNRS, Centrale Marseille, LMA, 13453 Marseille, France*

Abstract

Solar powered HALE drones pose further challenges in terms of aerodynamic and structural design. This results in highly flexible high aspect ratio composite wing particularly vulnerable to destructive fluid/structure interaction such as torsional divergence or flutter. The aims of this study is to enhance aeroelastic performance using the anisotropy of laminated composites, in particular bending/twisting coupling with a method called aeroelastic tailoring. For this purpose an appropriate simulation toolbox based on a reduced order model is presented. After showing some test cases, the influence of laminate plies orientation on aeroelastic performance is exposed on simple composite specimens.

1. Introduction

From the earliest days of aviation, aircraft undergo fluid/structure interactions like torsional divergence, flutter, limit cycle oscillation or buffeting.[1] The early aircrafts, because of their flexible airframe, were particularly exposed to these phenomena, as are concerned a new type of innovative aircraft, namely solar powered High Altitude Long Endurance (HALE) Unmanned Aerial Vehicles (UAV). Indeed, the low on-board power of the latter involve a high level of aerodynamic and structural performance. A good way to meet this objective is to design an aircraft with a high aspect ratio wing (enhanced lift-to-drag ratio) and a lightweight composite airframe (low wing loading).[2] This kind of aircraft is characterized by in-flight large deflection and large rotation of the wing involving an interaction between aerodynamic, structural mechanics and even flight mechanics on one hand and the need for a nonlinear approach on the other.

Figure 1: Wreckage of Helios on the 26th June 2003[3]

A famous example of this kind of interaction is the crash of the NASA solar powered UAV Helios on the 26th June 2003 (figure 1). The cause of the accident is due to large deflection of the wing leading to an unstable pitch oscillation mode.[3] The classical way to enhance the critical speed of these phenomena is to make the airframe structure stiffer at the expense of mass balance. This solution should be avoided in case of solar powered UAV because of the challenging weight objectives. Thus an alternative method called "aeroelastic tailoring" is investigated in the present

study.[4] Initially developed on the experimental NASA aircraft X29, it consists in using composite anisotropy in order to set a passive closed-loop control on these interactions.

In order to meet these challenging objectives, the present work aims to develop a simulation toolbox able to simulate nonlinear and anisotropic behavior of high aspect ratio composite wing. This tool is designed as an open source program in Fortran and Python sufficiently effective to be suitable for optimization purposes. In the second part of this paper, after providing a brief overview of existing nonlinear aeroelastic reduced order models, we will present the geometrically exact beam theory used to model airframe structure and the associated homogenization step. Then, we will talk about the unsteady strip theory used to compute aerodynamics forces applied to the wing. Part three contains the validation test cases conducted with the toolbox. We will finish with the study of a simple laminated composite wind tunnel specimen displaying different fiber orientations in order to demonstrate the relevancy of aeroelastic tailoring concept in high aspect ratio composite wing design.

2. Reduced order aeroelastic models

The nature of a fluid/structure interaction strongly depends on the system characteristics. Different approximations are made depending on the motion of structure relatively to the fluid. In order to quantify that, dimensionless number are used. In our case, the degree of fluid/structure coupling is characterized by the reduced frequency $f_r = T_f/T_s$ with T_f the period of fluid motion and T_s the period of structure motion.[5]

Solar powered HALE UAV, because of their large wingspan and their low flight speed (for instance 75 m wingspan and 35 km/h for Helios UAV), are characterized by a reduced frequency near 1. In fact, it means that the fluid "see" the motion of the structure and, conversely, the structure "see" the motion of the fluid. Therefore, high fidelity simulation of this kind of fluid structure/interaction with finite volume method coupled with a finite element method still leads to a prohibitive computational cost. Indeed, it implies an unsteady resolution of both problem (fluid and structure) and the transfer between fluid and solid of position and velocity informations. Consequently, aeroelastic reduced order model are still widely used, especially for highly flexible aircrafts.

We could mention some of the main nonlinear aeroelastic reduced order model already developed. Most of them rely on the aerodynamic part on inviscid, incompressible potential flow method. For medium aspect ratio wing, an effective solution selected for the computation code NANSI[6] is based on the Unsteady Vortex Lattice Method (UVLM) coupled with a nonlinear beam theory. A better suited method to high aspect ratio wing is used in the Drela program ASWING.[7] This highly flexible aircraft conception tool combines a nonlinear isotropic beam formulation with an unsteady lifting line theory. More recently, Shearer and Cesnik have developed a Matlab toolbox called UM/NAST (University of Michigan/ Nonlinear Aeroelastic Simulation Toolbox)[8] made up of a strain-based geometrically nonlinear beam formulation linked with a finite state two-dimensional incompressible flow aerodynamic theory proposed by Peters and al.[9] A similar formulation is used by Ribeiro in the Matlab toolbox Aeroflex.[10]

Most of these models use isotropic formulation, therefore do not enable the quantification of aeroelastic tailoring effects. It can be done using the Matlab toolbox proposed by Patil and Hodges called NATASHA (Nonlinear Aeroelastic Trim and Stability of HALE Aircraft).[11] This brief overview of existing models, linked to the specificities of solar powered HALE aircraft, shows a need for an efficient open source computation code (fitted for optimization processes) suitable to slender composite structures subject to unsteady aerodynamic forces.

2.1 Anisotropic beam theory

Aeroelastic tailoring consist in exploiting laminate composite anisotropy by setting a proper layup. For most applications, a laminate layup present a mirror symmetry with respect to its middle plane. If we consider a laminate plate of unidirectional (UD) plies, the layup [-45°,0°,45°,90°,90°,45°,0°,-45°], with angular values representing fiber orientation in each ply, presents a mirror symmetry. The aims of this type of symmetry is to dissociated membrane behavior (inplane loadings imply inplane displacements and vice versa) from bending behavior. It is especially useful to avoid the warping of a hot polymerized laminate plate during cool down. Another common rule concerning the UD plies orientation is to set balanced layup, namely to put for instance as many -45° plies as 45° plies. It is meant to avoid coupling between the different bending behavior.

The true principle of aeroelastic tailoring is to ignore these rules, thus allowing coupling between the different behaviors of the laminate. It mainly consist in creating a link between the bending and the warping of the laminate. On the aerodynamic side, it induces the coupling of the bending due to lift forces and the twisting of the wing which determines the local angle of attack. Thus, the aeroelastic tailoring is a way to establish a feedback loop on the aeroelastic behavior of a flexible aircraft (figure 2).

In that context, it is essential to ensure a proper modeling of the laminate anisotropy and geometrical non linearity. For this purpose, the choice fell on an open source tool named GEBT (Geometrically Exact Beam Theory) developed

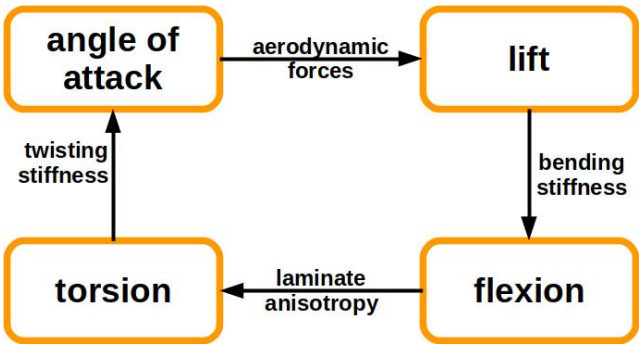

Figure 2: Principle of feedback loop induced by aeroelastic tailoring

by Yu and Blair designed for composite slender structures under large deflections and rotations, subject to the strains being small. This tool implements a mixed variational formulation based on exact intrinsic equations for dynamics of moving beams developed by Hodges.[12]

The exact intrinsic equations for dynamics are derived from Hamilton's weak principle asymptotically developed along the beam axes :

$$\int_{t_1}^{t_2} \int_0^L \left[\delta (K - U) + \overline{\delta W} \right] dx_1 dt \quad = \quad \overline{\delta A} \tag{1}$$

where t_1 and t_2 are arbitrary fixed times, K and U are the kinetic and strain internal energy, respectively, δ is the usual Lagrangian variation for a fixed time. $\overline{\delta W}$ is the virtual work of applied loads and $\overline{\delta A}$ the virtual action on the same period. The resulting formulation is detailled in Hodges.[12] The main asset of this type of method is to move away from coordinate system dependency (intrinsic nature) for the position and rotation parameters. Thus, it permits to avoid the non commutativity of rotation that occurs in case of large deflection. Kinematical and constitutive relations are then added to the weak formulation with Lagrange multipliers (mixed nature). The resulting formulation allow a finite element implementation with very simple shape functions (constant or linear).

The main capabilities of this computation code is to perform different type of simulation on variable-section composite slender structures :

- nonlinear static simulation;
- nonlinear steady-state dynamic simulation;
- nonlinear transient dynamic simulation;
- eigenvalue analysis of small motion about the steady-state by linearizing about the steady state.

For time computation purpose, all types of simulation can also be done in linear manner. This program is written in Fortran using well optimized libraries.

In this tool, cross sectional properties are inputs of the program. For all type of simulation, a symmetric flexibility matrix is needed to join the applied loads to the internal strain :

$$\begin{Bmatrix} \gamma_{11} \\ 2\gamma_{12} \\ 2\gamma_{13} \\ \kappa_1 \\ \kappa_2 \\ \kappa_3 \end{Bmatrix} = \begin{bmatrix} S_{11} & S_{12} & S_{13} & S_{14} & S_{15} & S_{16} \\ S_{12} & S_{22} & S_{23} & S_{24} & S_{25} & S_{26} \\ S_{13} & S_{23} & S_{33} & S_{34} & S_{35} & S_{36} \\ S_{14} & S_{24} & S_{34} & S_{44} & S_{45} & S_{46} \\ S_{15} & S_{25} & S_{35} & S_{45} & S_{55} & S_{56} \\ S_{16} & S_{26} & S_{36} & S_{46} & S_{56} & S_{66} \end{bmatrix} \begin{Bmatrix} F_1 \\ F_2 \\ F_3 \\ M_1 \\ M_2 \\ M_3 \end{Bmatrix} \tag{2}$$

where γ_{11} is the beam axial stretching strain measure, $2\gamma_{12}$ and $2\gamma_{13}$ are the engineering transverse shear strains, κ_1 is the twist measure, and κ_2 and κ_3 are the curvature measures. For dynamic simulation and eigenvalue analysis, we add the symmetric mass matrix as input :

$$\begin{Bmatrix} P_1 \\ P_2 \\ P_3 \\ H_1 \\ H_2 \\ H_3 \end{Bmatrix} = \begin{bmatrix} \mu & 0 & 0 & 0 & \mu x_{m3} & \mu x_{m2} \\ 0 & \mu & 0 & -\mu x_{m3} & 0 & 0 \\ 0 & 0 & \mu & \mu x_{m2} & 0 & 0 \\ 0 & -\mu x_{m3} & \mu x_{m2} & i_{22}+i_{33} & 0 & 0 \\ \mu x_{m3} & 0 & 0 & 0 & i_{22} & -i_{23} \\ -\mu x_{m2} & 0 & 0 & 0 & -i_{23} & i_{33} \end{bmatrix} \begin{Bmatrix} V_1 \\ V_2 \\ V_3 \\ \Omega_1 \\ \Omega_2 \\ \Omega_3 \end{Bmatrix} \tag{3}$$

where P_i and H_i are linear and angular momenta, V_i and Ω_i are linear and angular velocity, $i = 1, 2, 3$, μ is the mass per unit length, (x_{m2}, x_{m3}) is the location of mass center, i_{22} is the mass moment of inertia about axis 2, i_{33} is the mass moment of inertia about axis 3, i_{23} is the product of inertia. This formulation highlights the potential coupling between the different beam solicitations through non-diagonal coefficients of both matrix. For instance, the bending/twisting coupling mentioned on the figure 2 is enabled by a non-zero coefficient S_{45} or S_{46} (or both).

In case of an isotropic material, at its shear center, the flexibility is defined by :

$$\begin{bmatrix} \frac{1}{ES} & 0 & 0 & 0 & 0 & 0 \\ 0 & \frac{1}{GK_2} & 0 & 0 & 0 & 0 \\ 0 & 0 & \frac{1}{GK_3} & 0 & 0 & 0 \\ 0 & 0 & 0 & \frac{1}{GJ} & 0 & 0 \\ 0 & 0 & 0 & 0 & \frac{1}{EI_2} & 0 \\ 0 & 0 & 0 & 0 & 0 & \frac{1}{EI_3} \end{bmatrix} \tag{4}$$

where E is the Young modulus of the material, G its Coulomb modulus, S the cross-sectional area, I_2 and I_3 are area moment of inertia and K_2 and K_3 are shear coefficient in direction 2 and 3.

2.2 Homogenization step by volumetric finite element method

As seen previously, the flexibility matrix is easy to define for isotropic material with matrix (4), which is not true for an anisotropic one. In the latter case, different approaches are usable. We could mentioned analytical methods based on the Classical Laminate Theory (CLT), like for example the program Precomp[13] from the National Renewable Energy Laboratory (NREL) developed for wind turbine conception. This type of method presents a low computational cost but are accurate only for specific cross-sectional configuration. Along with CLT-based method, more complex approaches are developed like VABS program (Variational Asymptotic Beam Sectional Analysis).[14] This class of methods are accurate and efficient but are not freely accessible and cannot be integrated into an open source toolbox.

An alternative is to perform a volumetric finite element analysis and deducing the cross-sectional properties. This solution is more computationally intensive but is simpler to implement and allow any shape for the studied slender structure. The open source finite element code selected for this purpose is Calculix.[15] This one is particularly well suited to that homogenization step because it already treats beam problem by expanding beam elements into volumetric elements. To this end, it uses quadratic brick elements with reduced integration (C3D20R) particularly fitted for this application. The shape functions of the latter are rich enough to reproduce the behavior of an anisotropic slender structure with a limited number of elements.

Because of the high aspect ratio of the aircraft's wings studied, we make the Euler/Bernoulli assumption. As a consequence, coefficients of the second and third line (and thus second and third column by symmetry) of flexibility matrix (2) are equal to zero. Consequently it remains 16 coefficients to determine, it can be done using the further procedure :

- A piece of beam is defined with the proper cross-sectional and a length L ten times greater than the larger of the other two dimensions (avoiding edge effects).
- One side is clamped and the other is stiffened using "RIGID BODY" input card. A reference node is defined to represent beam translational and rotational degree of freedom and allowing the application of beam forces and bending moments.
- Four linear static calculations are made with different load cases applied on the reference node : the simple traction, the two pure bending and the simple torsion. The loading intensity is set to $1/L$ in order to simplify the identification step.
- Displacements of the reference node are measured for each load case. Because of the linear assumption, we can directly identify the displacement and rotation to the flexibility matrix coefficients.

For instance, the simple traction load case give this result :

$$\begin{Bmatrix} \gamma_{11} \\ 2\gamma_{12} \\ 2\gamma_{13} \\ \kappa_1 \\ \kappa_2 \\ \kappa_3 \end{Bmatrix} = \begin{bmatrix} S_{11} & S_{12} & S_{13} & S_{14} & S_{15} & S_{16} \\ S_{12} & S_{22} & S_{23} & S_{24} & S_{25} & S_{26} \\ S_{13} & S_{23} & S_{33} & S_{34} & S_{35} & S_{36} \\ S_{14} & S_{24} & S_{34} & S_{44} & S_{45} & S_{46} \\ S_{15} & S_{25} & S_{35} & S_{45} & S_{55} & S_{56} \\ S_{16} & S_{26} & S_{36} & S_{46} & S_{56} & S_{66} \end{bmatrix} \begin{Bmatrix} \frac{1}{L} \\ 0 \\ 0 \\ 0 \\ 0 \\ 0 \end{Bmatrix} \Rightarrow \begin{cases} L\gamma_{11} = S_{11} \\ L\kappa_1 = S_{14} \\ L\kappa_2 = S_{15} \\ L\kappa_3 = S_{16} \end{cases}$$

with $L\gamma_{11} = u_1$ the displacement along axis 1 and $L\kappa_i = w_i$ the rotation around axis i, $i = 1, 2, 3$. Thanks to the matrix symmetry, this method allows the determination of the 16 unknowns coefficients.

2.3 Two-dimensional aerodynamic forces implementation

The high aspect ratio assumption gives us the opportunity to neglect tridimensional effects and thus to use a strip theory which can be easily linked to a beam formulation. This implementation can be done in two different ways :

- A weak coupling consisting in defining the aerodynamic load to apply on the beam in accordance with position and speed parameters extracted form the last structural calculation. This method is easy to implement and is well suited for modular architecture like, for instance, computation code FAST from the NREL.[16] However, it also has its drawbacks like the inability to perform coupled eigenvalue analysis or some convergence issues for nonlinear Newton-Raphson algorithms (aerodynamic loads are not taken into account into the Jacobian matrix).
- A strong coupling done by integrating aerodynamic loads directly into the weak formulation of the beam theory. This approach is much more complex and is not really adapted to modular architecture but allows to overcome the main drawbacks of a weak coupling. Indeed, the most interesting application is the possibility to determine, for a particular flow velocity, the aeroelastic modes of the wing about a steady sate, namely frequencies, modal shapes and damping factors. The latter is a key parameter for our study because it defines the limit between stable and unstable speed and thereby provide the flutter boundary. Concomitantly, a zero-frequency mode for a given flow velocity indicates torsional divergence speed overrun.

Consequently, the strong coupling has been chosen for our toolbox. Several aerodynamic forces formulations are implemented. A quasi-steady model:[17]

$$L = 2\pi\rho bU\left[\dot{h} + b\left(\frac{1}{2} - a\right)\dot{\alpha} + U\alpha\right] \tag{5}$$

$$M = b\left(\frac{1}{2} + a\right)L - \frac{\pi\rho U b^3}{2}\dot{\alpha} \tag{6}$$

with L the linear lift, M the linear moment around a reference point F, ρ the air density and U the flow velocity. The semi-chord b, the height h, angle of attack α and parameter a are detailed in figure 3. The reference point F coincides with the reference point of the homogenization step.

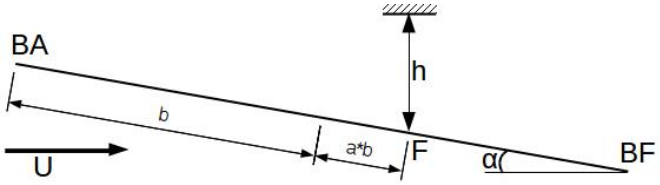

Figure 3: Airfoil parameters

This model is already implemented in the toolbox and should be completed by the finite state flow induced formulation of Peters[9] :

$$L = \pi\rho b^2\left(\ddot{h} + U\dot{\alpha} - ba\ddot{\alpha}\right) + 2\pi\rho Ub\left[\dot{h} + U\alpha + b\left(\frac{1}{2} - a\right)\dot{\alpha} - \lambda_0\right] \tag{7}$$

$$M = b\left(\frac{1}{2} + a\right)L - \pi\rho b^3\left[\frac{1}{2}\ddot{h} + u\dot{\alpha} + b\left(\frac{1}{8} - \frac{a}{2}\right)\ddot{\alpha}\right] \tag{8}$$

with λ_0 a parameter bind to the shed wake vorticity. Calculation of the latter is detailed in Peters et al.[9] The case $\lambda_0 = 0$ corresponds to a specific case of the unsteady formulation of Theodorsen[18] with coefficient $C(k)$ equal to 1 and is thereafter called quasi-steady with apparent mass model.[10]

3. Model validation

For a validation purpose, two test cases are detailed below. The first discusses the homogenization step and the second one concerns the aeroelastic critical speed determination.

3.1 Single-ply laminate plate homogenization

The first test case is divided into two parts dealing respectively with mesh convergence issues and a comparison between 3D finite elements and beam model performance.

The study is performed on a constant rectangular cross-sectional beam (1 meter width; 5 mm thick) made of an isotropic material (E = 72 GPa, ν = 0.3). We compare the flexibility matrix resulting from the homogenization step detailed in 2.2 with the analytical values presented in matrix (4). Finite elements calculation are done using C3D20R elements and are compared to standard quadratic brick elements C3D20. The results are presented in table 1.

Table 1: Mesh convergence of identification process

$L \times l \times e$	$10 \times 2 \times 2$		$10 \times 4 \times 4$		$50 \times 5 \times 5$		$50 \times 16 \times 6$	
Coefficient	C3D20	C3D20R	C3D20	C3D20R	C3D20	C3D20R	C3D20	C3D20R
$\frac{1}{ES}$	-0.53%	-0.03%	-0.52%	-0.01%	-0.07%	0.00%	-0.06%	0.01%
$\frac{1}{GJ}$	-6.50%	-3.79%	-5.73%	-1.98%	-2.99%	-1.59%	-1.81%	-1.49%
$\frac{1}{EI_{G2}}$	-1.95%	-1.03%	-1.70%	-0.85%	-0.81%	-0.69%	-0.79%	-0.69%
$\frac{1}{EI_{G3}}$	-0.80%	-0.28%	-0.74%	-0.18%	-0.22%	-0.15%	-0.21%	-0.14%

The mesh convergence is fast with satisfactory performance since 160 elements ($10 \times 4 \times 4$). Convergence towards $1/GJ$ is slower than others coefficients but the analytical reference is calculated using thin wall simplifying assumption ($J = (1/3)e^3 l$). Then, the gap is not necessarily attributable to the 3D finite elements calculation.

The second part of the test case consist in comparing on the same specimen ($10 \times 1 \times 0.005$ m) made of a single ply of UD , results of two types of simulation :

- an anisotropic beam model GEBT after the homogenization step presented before made on a $10 \times 4 \times 4$ mesh;
- a full 3D finite elements calculation done by Calculix conducted on the same mesh.

The single-ply specimen is made of T300/914 carbon epoxy with the following characteristics : E_l = 134 GPa, E_t = 10 GPa, ν_{lt} = 0.25, ν_{tl} = 0.0187 et G_{lt} = 4.2 GPa. In order to evaluate nonlinear capacities, applied loads are set to generate deflections of the same order of magnitude as specimen dimensions. Three load cases are performed on the central point of the free side:

- simple traction : F_3 = 1 kN;
- simple torsion M_1 = 5 kN·m;
- pure bending M_2 = 10 kN·m.

For each load case, we measured vertical displacement u_3, rotation along beam axis w_1, and rotation in the vertical plane w_2. Beam calculation is performed on 10 elements (as much as volumetric elements lengthwise for the 3D calculation). Results are presented in figure 4.

This set of test appears to be conclusive. Only simple torsion load case at 0° and bending load case at 90° show a slight difference which can be explain by the highly nonlinear nature of the 3D finite elements configuration.

3.2 Flutter speed of an isotropic wing

The second test case concerns the implementation of the aerodynamic forces into the weak formulation defined in GEBT and in particular the ability to predict the flutter speed. The reference value is extracted from the Aeroflex toolbox.[10] For comparison purposes, two isotropic wings will be studied :

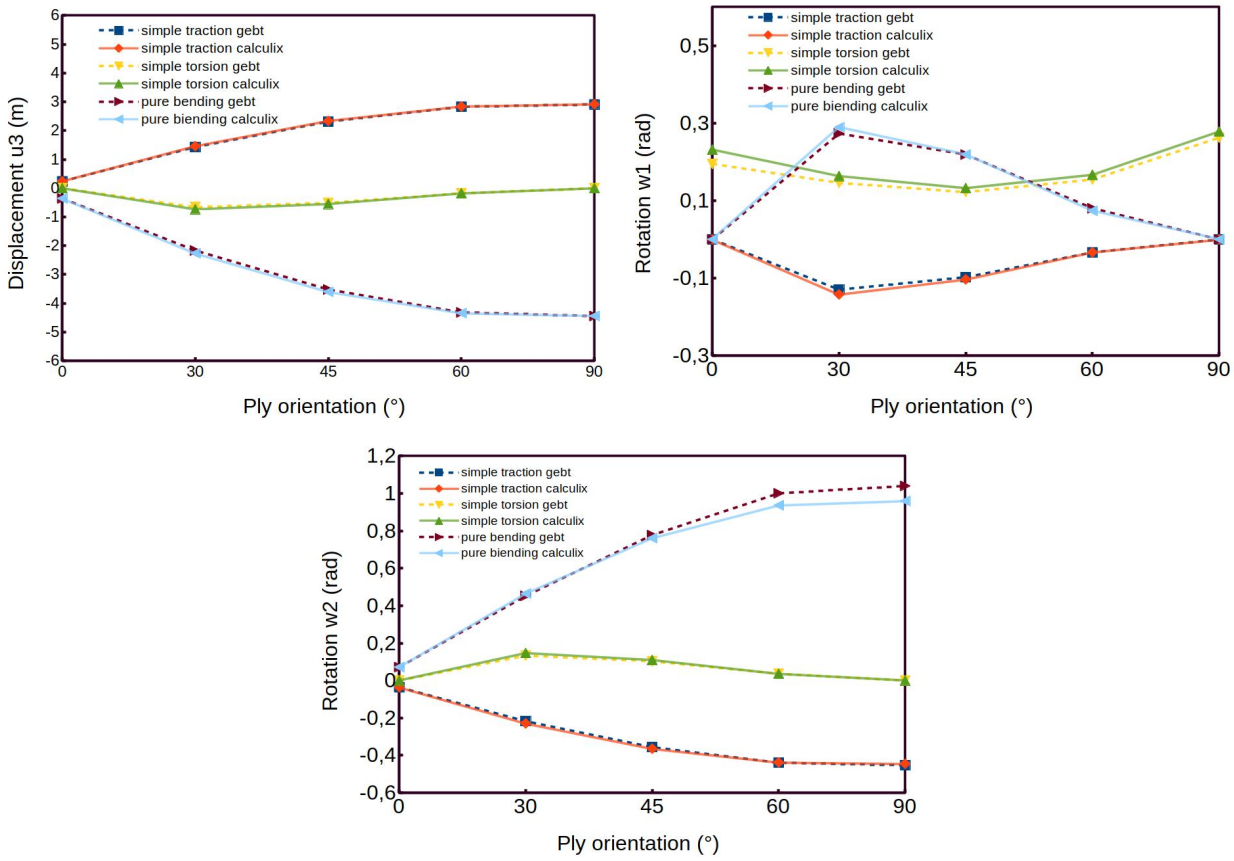

Figure 4: Comparison between GEBT computation code and Calculix results

- the medium aspect ratio Goland wing which is a widely used aeroelastic benchmark;[19]
- a high aspect ratio flexible wing inspired by the human powered aircraft Deadalus proposed by Patil.[20]

Characteristics are listed in table 2.

Table 2: Characteristics of Goland and Patil wings

	Goland	Patil
Semi-span L	6.096 m	16 m
Chord $2b$	1.8288 m	1 m
Mass per unit length μ	35.71 kg/m	0.75 kg/m
Elastic axis (from leading edge)	33 % chord	50 % chord
Center of gravity (from leading edge)	43 % chord	40 % chord / 45 % chord
Distance between CG and EA v	0.18288 m	−0.1 m / −0.05 m
Bending stiffness EI_{G2}(span-wise)	9.77×10^6 N.m^2	2.10^4 N·m^2
Bending stiffness EI_{G3}(chord-wise)	/	4.10^6 N·m^2
Torsional stiffness GJ	0.99×10^6 N·m^2	1.10^4 N·m^2
Mass moment of inertia around e.a. i_{11}	8.64 kg·m	0.10 kg·m

A simple way to modify the flutter speed is to move the position of the center of gravity while keeping the same flexibility and rotation inertia. Simulation are performed on both computation code (GEBT+aero and Aeroflex) with the two aerodynamic models (quasi-steady and quasi-steady with apparent mass) on 20 beam elements. Concerning GEBT inputs, the reference point is set on the elastic axis allowing the use of isotropic flexibility matrix (4). The mass

matrix is completed as follow :

$$\begin{bmatrix} \mu & 0 & 0 & 0 & 0 & \mu v \\ 0 & \mu & 0 & 0 & 0 & 0 \\ 0 & 0 & \mu & -\mu v & 0 & 0 \\ 0 & 0 & -\mu v & i_{11} & 0 & 0 \\ 0 & 0 & 0 & 0 & 0 & 0 \\ \mu v & 0 & 0 & 0 & 0 & i_{11} \end{bmatrix}$$

with v the distance between the center of gravity and the elastic axis and i_{11} the mass moment of inertia around elastic axis as mentionned on table (2). $i_{11} = i_{22} + i_{33}$ thus i_{22} is set to zero and $i_{33} = i_{11}$ because inertia around the spanwise bending is negligible.

The same method is followed to find the flutter speed by both program, namely it looks for the slowest flow velocity for which a negative damping exists. Results are presented in table 3.

Table 3: Flutter speed comparison between GEBT+aero and Aeroflex

Center of gravity		quasi-steady			quasi-steady with apparent mass		
(% chord from l.e.)		Aeroflex	gebt+aero	relative difference	Aeroflex	gebt+aero	relative difference
Goland wing	43 %	35.5885	35.1185	−1.32 %	64.7506	63.9192	−1.28 %
Patil wing	40 %	14.8553	14.8556	0.002 %	25.8021	26.4341	2.45 %
	45 %	6.2312	6.2294	−0.03 %	14.7777	15.0257	1.68 %

Results given by both programs are very close, especially for Patil wing with quasi-steady aerodynamics forces. Minor variations could be explained by the difference in the beam model employed.

4. Bending/twisting coupling influence on aeroelastic performance

Since test cases below are convincing, we are now looking for influence of fiber orientation on aeroelastic performance. For the purpose of a future wind tunnel campaign, we are looking for critical speed of simple composite laminate specimen. The square test section of the wind tunnel to be used is 45 cm wide, thus we will limit the length of specimen to 30 cm in order to minimize side-effects. In order to have a high aspect ratio (30) the chord is set to 2 cm. The material is the carbon epoxy described in paragraph 3.1. The layup is composed by 3 plies (0.25 mm thick), orientated at 45° at the bottom, 0° in the middle and variable at the front. A simulation is done every 15°

Since the orientation of front ply affects the stiffness of specimens, we also mentioned values of S_{44} and S_{55} coefficients which represents respectively torsional flexibility and bending flexibility. Results are presented on figure 5.

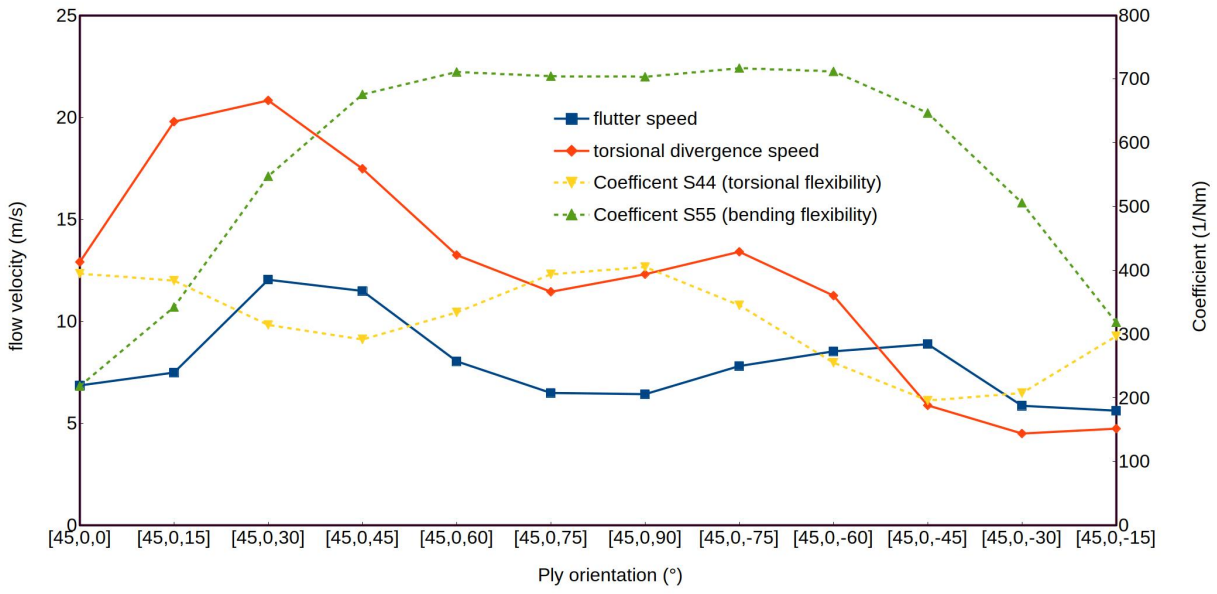

Figure 5: Influence of fiber orientation on aeroelastic critical speeds

It can be stated that the variation of a single ply orientation in a 3-ply specimen has a clear impact on critical speeds (torsional divergence and flutter). Another interesting fact is that best results are not obtain for the stiffer layup because the optimal aeroelastic configuration is obtain for a layup close to $[45°, 0°, 30°]$ (which is not balanced and without mirror symmetry) whereas stiffer specimens range from $[45°, 0°, -45°]$ to $[45°, 0°, 0°]$ layups.

5. Conclusion

Innovative concept of solar powered HALE aircraft imposes a careful study of aeroelastic phenomena on the understanding that consequences of those are often dramatic. This kind of studies has to take into account nonlinear effects because of large deflections and large rotations of flexible wing and the anisotropy of composite laminate material that constitute it. The anisotropy is in fact a mean to postpone aeroelastic critical speeds without detriment to the lightness of the airframe by using a proper orientation of UD in the laminate layup.

The aim of the present work is to build an efficient simulation toolbox able to catch the aeroelastic behavior of this category of aircraft by coupling in a reduced order model a nonlinear anisotropic beam formulation (GEBT) with an unsteady aerodynamic strip theory. After presenting validation test cases, a first set of simulation is carried out on simple composite laminate specimens intended for a wind tunnel test campaign. The results highlight the significant influence of plies orientation on aeroelastic behavior. Despite the simplicity of studied specimens (constant cross-sectional with 3 plies), the prediction of optimal aeroelastic performance seems to be complex and point out the need for an optimization process.

References

[1] Earl H. Dowell, éditeur. *A Modern Course in Aeroelasticity*, volume 116 de *Solid Mechanics and Its Applications*. Kluwer Academic Publishers, Dordrecht, 2005.

[2] O. Montagnier et L. Bovet : Optimization of solarpowered HALE UAV. *In Proc. 2nd Int. Congress of the Aeronautics Science, ICAS 2010, Cancun*, 2010.

[3] Thomas E. Noll, John M. Brown, Marla E. Perez-Davis, Stephen D. Ishmael, Geary C. Tiffany et Matthew Gaier : Investigation of the Helios prototype aircraft mishap. 9, 2004.

[4] Mayuresh J. Patil : Aeroelastic tailoring of composite box beams. *In Proceedings of the 35th Aerospace Sciences Meeting and Exhibit*, pages 97–0015, 1997.

[5] Pascal Hemon : *Vibrations des structures couplees avec le vent*. Editions Ecole Polytechnique, 2006.

[6] Zhicun Wang, P. C. Chen, D. D. Liu et D. T. Mook : Nonlinear-aerodynamics/nonlinear-structure interaction methodology for a high-altitude long-endurance wing. *Journal of Aircraft*, 47(2):556–566, 2010.

[7] Mark Drela : Integrated simulation model for preliminary aerodynamic, structural, and control-law design of aircraft. *AIAA Paper*, 99:1394, 1999.

[8] Christopher M. Shearer et Carlos ES Cesnik : Nonlinear flight dynamics of very flexible aircraft. *Journal of Aircraft*, 44(5):1528–1545, 2007.

[9] David A. Peters, Swaminathan Karunamoorthy et Wen-Ming Cao : Finite state induced flow models. I-Two-dimensional thin airfoil. *Journal of Aircraft*, 32(2):313–322, 1995.

[10] Flavio Luiz Cardoso Ribeiro, Pedro Paglione, Roberto Gil Annes da Silva et Marcelo Santiago de Sousa : Aeroflex: a toolbox for studying the flight dynamics of highly flexible airplanes. 2012.

[11] C.-S. Chang, Dewey H. Hodges et Mayuresh J. Patil : Flight dynamics of highly flexible aircraft. *Journal of Aircraft*, 45(2):538–545, 2008.

[12] Dewey H. Hodges : A mixed variational formulation based on exact intrinsic equations for dynamics of moving beams. *International journal of solids and structures*, 26(11):1253–1273, 1990.

[13] Gunjit S. Bir : *User's guide to PreComp (pre-processor for computing composite blade properties)*. National Renewable Energy Laboratory, 2006.

[14] Carlos ES Cesnik et Dewey H. Hodges : VABS: a new concept for composite rotor blade cross-sectional modeling. *Journal of the American Helicopter Society*, 42(1):27–38, 1997.

[15] G. Dhondt et K. Wittig : Calculix: a free software three-dimensional structural finite Element Program. *MTU Aero Engines GmbH, Munich, Germany*, 1998.

[16] Jason M. Jonkman et M. L. Buhl Jr : FAST User s Guide, National Renewable Energy Laboratory. *No. NREL/EL-500-38230, Golden, CO*, 2005.

[17] H. Haddadpour et R. D. Firouz-Abadi : Evaluation of quasi-steady aerodynamic modeling for flutter prediction of aircraft wings in incompressible flow. *Thin-walled structures*, 44(9):931–936, 2006.

[18] Theodore Theodorsen : General theory of aerodynamic instability and the mechanism of flutter. 1935.

[19] Martin Goland : The flutter of a uniform cantilever wing. *Journal of Applied Mechanics-Transactions of the Asme*, 12(4):A197–A208, 1945.

[20] Mayuresh J. Patil : *Nonlinear aeroelastic analysis, flight dynamics, and control of a complete aircraft*. Thèse de doctorat, Citeseer, 1999.